Comparison of dynamic and quasi-static measurements of thin film adhesion

2011 J. Phys. D: Appl. Phys. 44 034006

(http://iopscience.iop.org/0022-3727/44/3/034006)

J. Phys. D: Appl. Phys. **44** (2011) 034006 (8pp) doi:10.1088/0022-3727/44/3/034006

Comparison of dynamic and quasi-static measurements of thin film adhesion

Phuong Tran[1], Soma S Kandula[2], Philippe H Geubelle[2] and Nancy R Sottos[3]

[1] Department of Mechanical Science and Engineering, University of Illinois at Urbana-Champaign, Urbana, IL, USA
[2] Department of Aerospace Engineering, University of Illinois at Urbana-Champaign, Urbana, IL, USA
[3] Department of Materials Science and Engineering, University of Illinois at Urbana-Champaign, Urbana, IL, USA

Received 9 July 2010, in final form 29 September 2010
Published 22 December 2010
Online at stacks.iop.org/JPhysD/44/034006

Abstract
Adhesive failure and the attendant delamination of a thin film on a substrate is controlled by the fracture energy required to propagate a crack along the interface. Numerous testing protocols have been introduced to characterize this critical property, but are limited by difficulties associated with applying precise loads, introducing well-defined pre-cracks, tedious sample preparation and complex analysis of plastic deformation in the films. The quasi-static four-point bend test is widely accepted in the microelectronics industry as the standard for measuring adhesion properties for a range of multilayer thin film systems. Dynamic delamination methods, which use laser-induced stress waves to rapidly load the thin film interface, have recently been offered as an alternative method for extracting interfacial fracture energy. In this work, the interfacial fracture energy of an aluminium (Al) thin film on a silicon (Si) substrate is determined for a range of dynamic loading conditions and compared with values measured under quasi-static conditions in a four-point bend test. Controlled dynamic delamination of the Al/Si interface is achieved by efficient conversion of the kinetic energy associated with a laser-induced stress wave into fracture energy. By varying the laser fluence, the fracture energy is investigated over a range of stress pulse amplitudes and velocities. For lower amplitudes of the stress wave, the fracture energy is nearly constant and compares favourably with the critical fracture energy obtained using the four-point bend technique, about 2.5 J m^{-2}. As the pulse amplitude increases, however, a rate dependence of the dynamic fracture energy is observed. The fracture energy increases almost linearly with pulse amplitude until reaching a plateau value of about 6.0 J m^{-2}.

(Some figures in this article are in colour only in the electronic version)

1. Introduction

Interfacial adhesion is an important factor influencing the mechanical reliability of multilayered microelectronic devices, since failure often occurs at interfaces between dissimilar thin film layers when the device is subjected to thermo-mechanical loading. Accurate characterization of thin film interfacial adhesion is essential to the development of predictive models for delamination and interface degradation. A number of quasi-static test methods have been devised to measure thin film adhesion including peel, stud-pull, scratch, blister, indentation and four-point bend tests [1, 2]. Among those test protocols, the four-point bend technique is often preferred in the microelectronics industry for measurement of the critical interfacial debonding energy G_c [3, 4].

In the four-point bend technique, the film stack of interest is sandwiched between two elastic Silicon (Si) substrates to prevent stress relaxation and plastic deformation during the interfacial debonding process [2]. The two substrates are bonded together by an epoxy layer (figure 1(*a*)). A central notch is introduced on the top of a substrate to serve as a pre-crack. The multilayer system is then subjected to a symmetric four-point bend loading at a slow, controlled rate to initiate a crack at the notch tip. The crack propagates through the

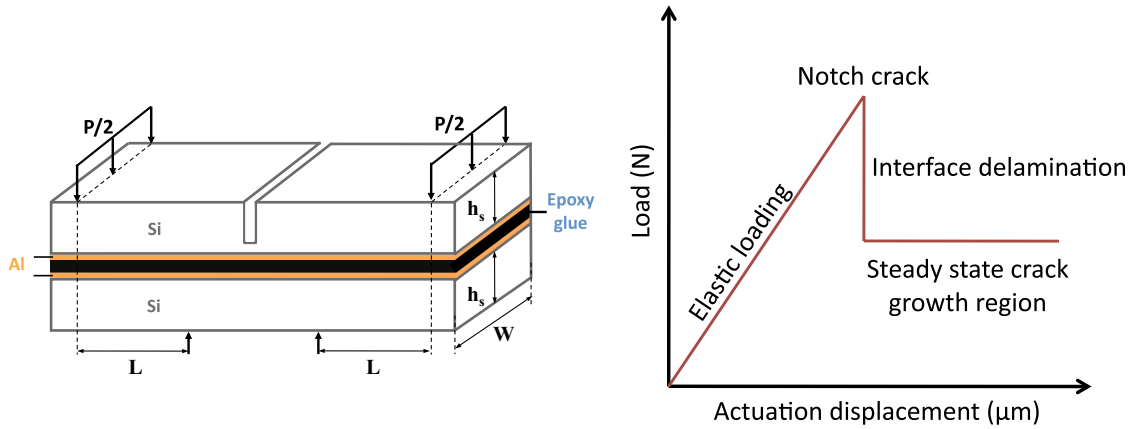

Figure 1. (*a*) Schematic of four-point bend sample geometry. (*b*) Schematic load–displacement curve during four-point bend test, the interface fracture energy is calculated based on the load value measured at the plateau region.

thickness of the Si substrate leading to a sharp drop in the load–displacement curve (figure 1(*b*)). In a successful test, the crack arrests at the thin film/substrate interface and then proceeds to delaminate the film as indicated by the plateau region in the load–displacement curve. The steady-state value of the energy release rate G, first derived in [5], is the fracture toughness G_c of the interface. The effectiveness and repeatability of the four-point bend test relies on generation and propagation of a pre-crack along the interface of interest. In particular, the use of the four-point bend test in industrial applications has faced a significant challenge as the crack, in many cases, does not deflect into the interface of interest [4]. The success of the four-point bend test is strongly dependent on the sample preparation process and testing procedure. Key variables include the substrate and bonding materials, thickness of adhesive layer, notch depth, loading rate, sample dimensions, pin spacing and edge polishing.

In contrast to quasi-static methods, laser-spallation-based techniques provide non-contact, dynamic loading of the thin film/substrate interface with a laser-induced, high-amplitude acoustic pulse [6–10]. A nearly 1D, compressive, longitudinal wave packet is generated on the back side of the substrate with a temporal shape similar to the laser pulse and propagates through the substrate towards the film/substrate interface. Upon reaching the free surface of the thin film, the stress pulse reflects and loads the interface in tension at very high strain rates ($\sim 10^7\ s^{-1}$). At a critical stress level, the interface fails and the film spalls from the substrate. This spallation protocol has been used to characterize the tensile and mixed-mode strength of a wide range of thin film interfaces [9, 11–17]. Beyond the application to interface strength measurement, more recent research has also aimed at applying the laser-spallation technique to quantify the interfacial fracture energy [18, 19]. This experimental method relies on the ability to harness the kinetic energy associated with the laser-induced stress pulse to initiate failure and propagate a crack along the interface. Early experiments and numerical simulations of the dynamic delamination of patterned thin films [20] have revealed the important role of inertia in achieving a controlled crack propagation process. More recent efforts [18, 21] exploit this inertial effect and enhance the efficiency of the laser-induced interface delamination technique by optimizing the specimen geometry and material selection. A schematic of this experiment is shown in figure 2(*a*). Patterned thin films are deposited on a silicon substrate. A weak adhesive layer introduced beneath the patterned film serves as pre-crack during the rapid dynamic loading event. The kinetic energy trapped in the weak adhesion portion of the film is proportional to the length of the pre-crack and serves as the driving force for substantial crack extension.

In this paper, we compare the fracture energy extracted from the dynamic delamination experiments with the value obtained from the quasi-static four-point bend tests on the Al/Si interface. The results provide insight into the effect of loading rate and mode-mixity on the interfacial adhesion measurement.

2. Dynamic delamination experiment

Thin film delamination specimens (figure 2(*a*)) are produced by depositing on a Si (1 0 0) substrate a 310 μm wide, 380 μm long, and 250 nm thick gold (Au) rectangular film as a weak adhesion layer followed by a 310 μm wide and 2.8 or 3.8 μm thick Al film strip. The Al test films are deposited over the length of 20 mm and separated by 2 mm from each other to ensure the negligible interference with dynamic loading.

A Nd : YAG laser pulse of wavelength 1064 nm with a nominal beam size of 3.5 mm is focused to a spot of 1.5 mm on the absorbing layer, which is sandwiched between the back side of the substrate and the waterglass constraining layer. The incident laser pulse causes a melting-induced expansion of the Al absorbing layer on the back side of the Si substrate. The rapid expansion of the Al film is confined by a layer of waterglass, generating a near Gaussian-shaped acoustic compressive stress wave with a rise time of $\simeq$5 ns. A finely focused probe beam from an argon ion laser ($\lambda = 514.5$ nm) is used to precisely align the Nd : YAG laser pulse beam with the weak adhesion region prior to the adhesion test. The probe beam also forms one arm of a Michelson interferometer for measurement of the out-of-plane displacement of the substrate during the spallation test. The loading substrate pulse information is extracted by correlating the interferometric fringe intensity pattern with the out-of-plane displacement of the substrate (figure 2(*b*)). The reflected tensile wave from the

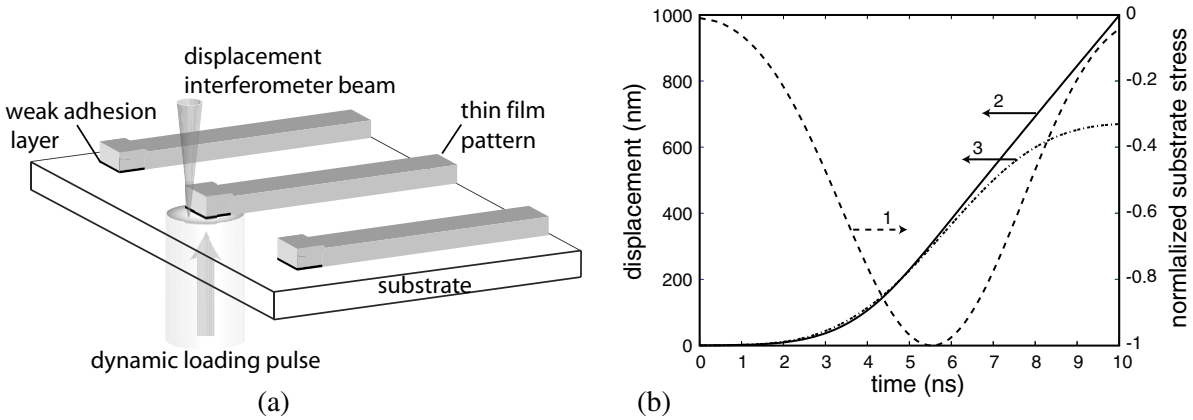

Figure 2. (*a*) Schematic of the dynamic adhesion test. (*b*) Measured substrate stress pulse normalized by its amplitude (1) and corresponding experimental displacement histories of the weakly (2) and strongly bonded (3) portion of the thin film [18].

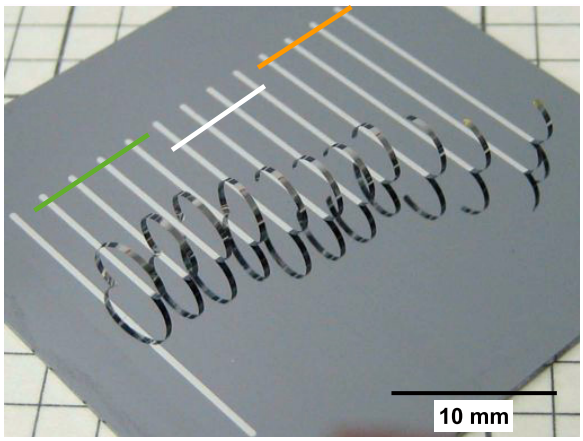

Figure 3. Successful laser-induced delamination of Al film patterns from a Si substrate. The final crack length a_f ranges from 4 to 8 mm with increasing laser fluence for an initial pre-crack length of 310 μm and a film thickness of 3.8 μm. The three solid lines indicate different sets of film strips tested at the same laser fluence. The upper-right solid line corresponds to the lowest fluence and the lower-left to the highest.

free surface of the film stack fails the weakly adhered Au/Si interface instantaneously to form a pre-crack. The kinetic energy trapped in the debonded portion of the film serves as the driving force for the subsequent crack extension.

We tested identical thin film strips at increasing laser fluence levels ranging from 20 to 75 mJ m^{-2}. The corresponding stress pulse amplitude was determined from interferometric measurements and ranged from 0.55 to 1.8 GPa. Successful delamination of the patterned thin Al films is shown in figure 3. Remarkable final crack extensions are obtained, some exceeding 10 mm, which is nearly 30 times greater than the length of the initial weak adhesion layer. Excellent repeatability was obtained at each fluence level tested.

The analysis to extract the thin film interface toughness is based on the hypothesis that the dynamic delamination event is driven entirely by the inertial energy imparted to the film by the stress pulse loading. We calculate the interface toughness G_c by balancing the kinetic energy trapped in the thin film at the onset of spallation of weak interface of length a_0 (pre-crack length), with the energy required for final crack extension $a_f - a_0$, through the simple relation

$$G_c = \frac{a_0 K_{1D}}{a_f - a_0}, \tag{1}$$

where K_{1D} denotes the kinetic energy available for the fracture process. The value of K_{1D} is obtained by assuming the spallation process of the weak adhesion layer takes place predominately under 1D conditions. The information of the loading substrate stress profile combined with the specimen geometry and material properties provides the necessary input for a 1D elastodynamic finite element simulation. The value of K_{1D} is calculated at the onset of spallation of the film above the weak adhesion region. Figures 4(*a*) and (*b*) show the effect of substrate pulse on K_{1D} and the final crack extensions for a 3.8 μm thick Al film, respectively. The error bars on the K_{1D} values account for a 5% experimental error in the estimation of the substrate pulse amplitudes. An increase in K_{1D} provides more energy for fracture and therefore greater crack extensions. The final shapes of the delaminated films in figure 3 indicate the presence of residual stress gradients. The estimation of the energy release rate associated with residual stress and stress gradient presented in [21] reveals that these energy components are substantially (two to three orders of magnitude) smaller than the measured critical fracture energy of the interface.

The reliability of equation (1) in calculating the fracture toughness has been investigated through systematic parametric studies [21]. The simulation of patterned film delamination in [21] reveals that for a particular dynamic test configuration of a 300 μm long pre-crack and 4 μm thick film, subjected to a pulse loading of 1.5 GPa in amplitude, more than 95% of kinetic energy imparted to the film from the stress pulse is converted into the failure process.

3. Four-point bend experiment

The four-point bend specimen preparation is shown schematically in figure 5. Samples consisted of two identical 500 μm thick rectangular Si (1 0 0) beams with dimensions 10 $\times$ 60 mm^2. The Si beams were pre-cut by a dicing saw

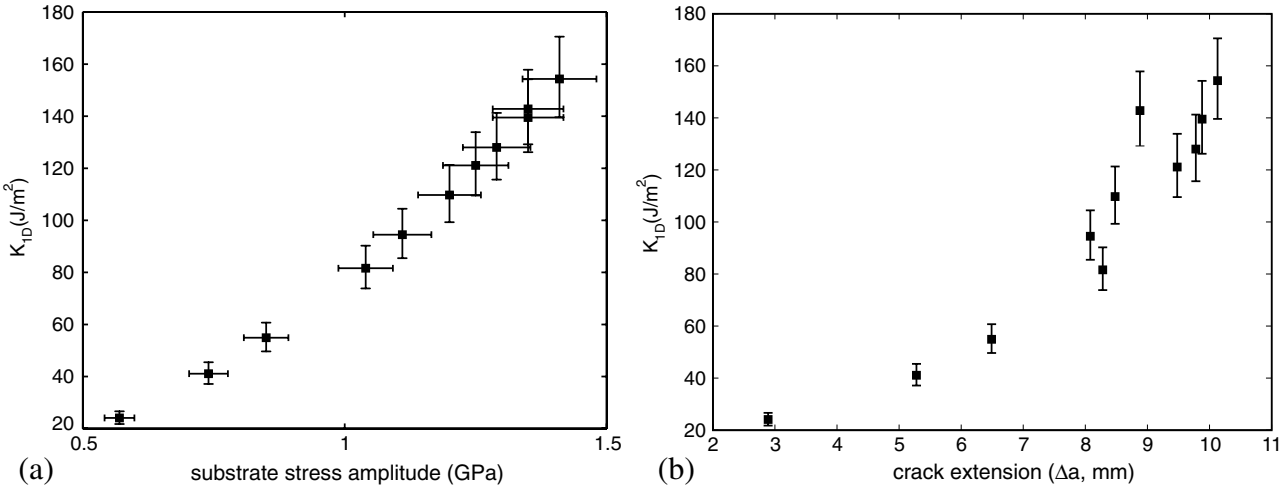

Figure 4. (*a*) Kinetic energy available for fracture, K_{1D}, as a function of the loading substrate pulse amplitude. (*b*) K_{1D} as a function of final interface crack extensions, Δa. The error bars in K_{1D} account for a 5% experimental variation in the substrate pulse amplitudes.

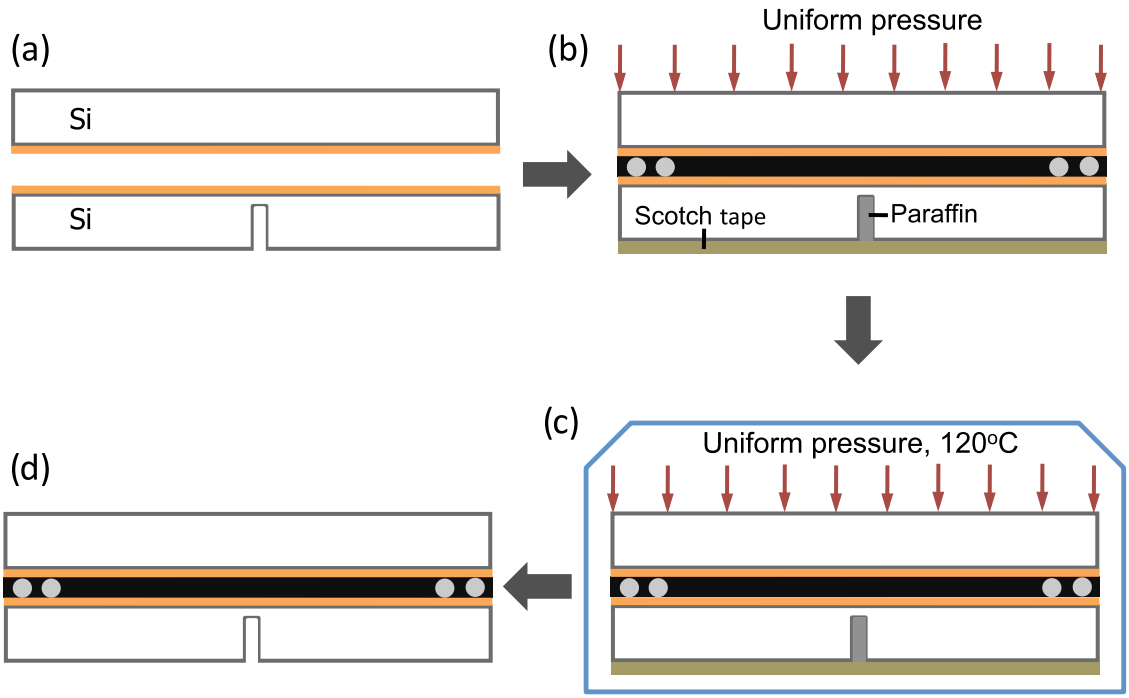

Figure 5. Sample preparation sequence: (*a*) Al thin film is evaporated on Si beam substrates, (*b*) Si beams are bonded together with epoxy using glass beads to control the thickness of adhesive layer, (*c*) samples are cured in the oven at 120 °C for 1 h, (*d*) samples are cleaned and polished for testing.

to provide samples of uniform sizes to assist the sample alignment process and narrow notches to achieve higher stress concentration at the notch tip to avoid overloading. A 80 μm wide notch was machined into one of the Si beam to a depth 75% of its thickness. The silicon beam surfaces were then gently cleaned by acetone, IPA and DI water, before the thin film deposition process. A 500 nm thick Al film was evaporated on to each Si beam. A thin layer of epoxy (Epoxy Bond 110, Allied High Tech) was then applied to Al surfaces to bond the two beams.

As shown in figure 5(*b*), glass spheres with diameters ranging from 10 to 15 μm were used as spacers to ensure a uniform thickness of the epoxy layer. The glass spheres were placed only at the edges of the epoxy layer outside the active bending region of the specimen (beyond the outer pins). Scotch tape and paraffin wax were used to seal the notched and side surface of the Si beam to prevent epoxy from penetrating the notch area. The specimens were then cured at 120 °C for 1 h under a compressive stress of ~0.016 N mm^{-2} to restrict any relative sliding between two Si substrates. Prior to testing, the edges of each specimen were carefully polished to remove epoxy residues and defects. The multiple layers of the sandwiched beam are visible in the polished cross-section in figure 6.

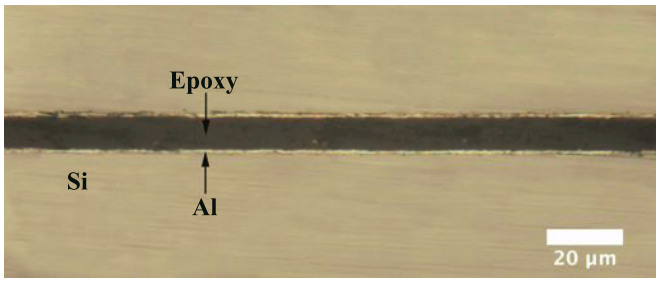

Figure 6. Image of specimen prior to testing.

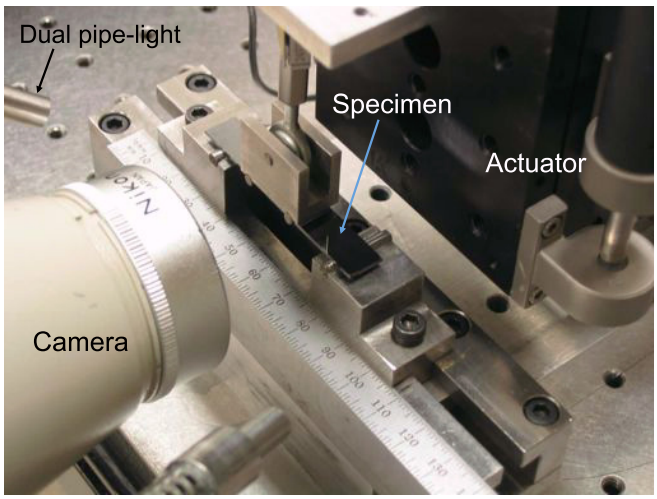

Figure 7. Experimental setup for the four-point bend test.

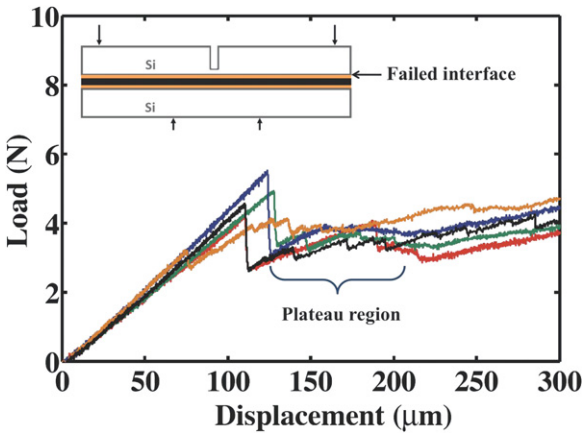

Figure 8. Representative load–displacement curves for five specimens. The average plateau force is calculated just after fracture initiation (in the range from 125 to 200 μm).

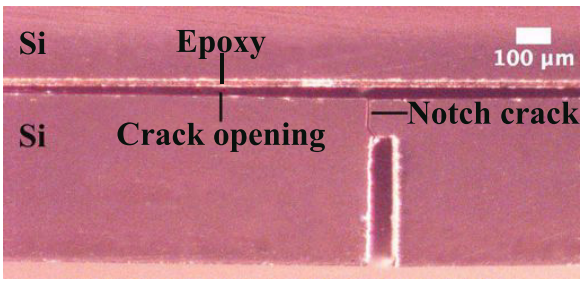

Figure 9. Image of delaminated specimen after testing.

The four-point bend apparatus is shown in figure 7. The upper span of the fixture had a fixed spacing of 16 mm, while the span of the lower fixture was adjustable. Preliminary testing was carried out for a range of span lengths on the lower fixture, and we determined that a spacing of 15 mm provided stable crack growth. The specimen was loaded at a rate of 0.1 μm s^{-1} as suggested in [3, 22] using a piezo linear actuator. The load was recorded by a load cell and a high resolution CCD camera imaged the beam deformation and crack extension during the test.

Figure 8 shows the load–displacement curves for five specimens. The initial slope of these curves indicates the stiffness of the specimen prior to failure. Upon reaching a critical load of 4 to 6 N, a crack is initiated at the notch tip, leading to a sharp load drop. The variations in the initial stiffness and critical load are attributed to the presence of a small amount of epoxy residue in the notch and slight differences in specimen geometry after the polishing step. The crack arrests at the Al film and generates a delamination along the Si/Al interface. A long plateau in the load occurs as the film delamination reaches an equilibrium state between the interface debonding process and specimen deformation. In the later stage of the failure process, an increase in the load occurs when the interface crack has reached the inner pins. The fracture toughness value of the Al/Si interface is extracted from the plateau region. For a specimen made of identical substrate material and assuming that the interfacial debond length is much greater than the thickness h_s of the substrate, the value of G_c is given by [5] as

$$G_c = \frac{21(1-\nu_s^2)M^2}{4E_s h_s^3}, \tag{2}$$

where $M = PL/2W$ is the bending moment per unit width, E_s is the elastic modulus of the substrate, ν_s, its Poisson's ratio, P, the critical force measured in the plateau region, L defines the pin spacing and W is the specimen width (figure 1(a)). The debond length does not enter into the calculation, which greatly simplifies the test. The critical load P is obtained by averaging load values along the plateau region.

As shown in figure 9, a vertical crack initiated from one corner of the notch. The tough epoxy layer prevented the crack from propagating through the entire sample, resulting in the delamination of the Al/Si interface. Three batches of 15 specimens taken from different wafers were tested. The average fracture energy calculated from equation (2) for these specimens is 2.5 ± 0.3 J m^{-2}. The standard deviation is within 12% of the measured value, which is consistent with the literature benchmarks [23].

4. Comparison of quasi-static and dynamic interfacial fracture energy

The interface fracture toughness obtained from the dynamic thin film delamination protocol is summarized in figure 10 for film thicknesses of 2.8 and 3.8 μm. The fracture energy values are not constant and vary between 2.5 and 6 J m^{-2},

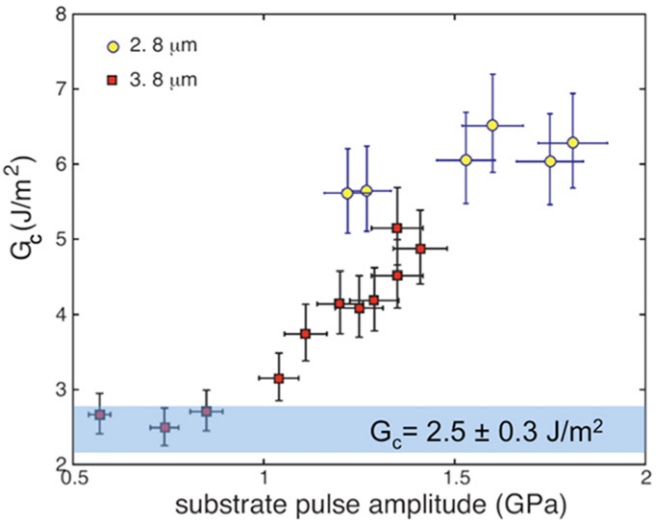

Figure 10. Comparison of fracture toughness obtained by the dynamic test with two values of the film thickness (symbols) and with the quasi-static four-point bend test. The shaded window indicates the range of values measured by the four-point bend technique. The error of the fracture toughness value is calculated as one standard deviation from a set of 13 successful tests.

corresponding to a variation of the substrate pulse amplitude from 0.5 to 2 GPa. The results from the quasi-static four-point bend experiments are also included in figure 10. At low stress pulse amplitudes, the interface fracture energy of the 3.8 μm thick film determined by dynamic testing is nearly constant and compares favourably with the quasi-static value of 2.5 J m^{-2} (shaded region). As the pulse amplitude increases, the dynamic fracture energy also increases until reaching a plateau of about 6 J m^{-2}. We hypothesize that the observed dependence on pulse amplitude is due to the influence of the loading rate and mode-mixity of the dynamic test. The adhesion energy is therefore represented as

$$G_c = G_c(V_0, \psi), \tag{3}$$

where V_0 denotes the peeling velocity at which the weak adhesion portion of the film is spalled from the substrate, and the phase angle ψ defines the mode-mixity of the failure event [24]. In the dynamic test, there is a direct correlation between the stress pulse amplitude σ_0 and the peeling velocity V_0,

$$V_0 = \sqrt{\frac{2K_{1D}}{\rho_f H_f}} \propto \frac{\sigma_0}{\rho_f c_d}\sqrt{\frac{1}{H_f}\int_0^{H_f} f^2(y)\,dy}, \tag{4}$$

where H_f, ρ_f and c_d are film thickness, density and dilatational wave speed in the film, respectively. The function f describes the spatial distribution of stress across film thickness at the onset of the pre-crack formation and is given in [20]. The peeling velocity V_0 is computed from a simple 1D wave propagation simulation for a given stress pulse [21]. For pulse amplitudes varying from 0.5 to 2 GPa, the corresponding values of V_0 range from 100 to 200 m s^{-1}. As the film is peeled from the interface at a high velocity, rate-dependent effects associated with the viscoplastic response of bulk material (Al) or the rate-sensitivity of interface may be activated [25–28]. Muralidhar and Sunil [26] have developed a numerical model combining a viscoelastic model for the bulk response and a rate-dependent cohesive model for the interface to simulate the influence of loading rate on the steady-state crack propagation between a rigid substrate and a thin viscoelastic film. This study has shown that the computed interfacial fracture energy falls into one of the three distinct regions depending on the peeling velocity. In the low velocity region, the viscous zone was very small leading to very little dissipation, and therefore the fracture energy was identical to the intrinsic fracture energy. At intermediate velocities, the energy was dissipated, as a result of the interaction between cohesive and viscous zones, almost proportional to the peeling velocity. For high peeling velocities, the viscous zone extended beyond the cohesive zone leading to the maximum energy dissipation, which was independent of peeling velocity. Hence, the low pulse amplitude in fracture energy in figure 10 may be associated with small amounts of energy dissipation, while the high-amplitude plateau may be associated with a size-limited dissipation zone. The difference in measured fracture toughness values for the 2.8 and 3.8 μm thick film (at a load amplitude of 1.4 GPa) could be attributed to the influence of the peeling velocity as described in equation (4) and the variation in sample preparation.

There is extensive literature [2, 29–31] supporting the dependence of fracture toughness on the mode-mixity of the failure process. This effect is explained by either frictional interaction or the change in size and shape of energy-dissipation zone at the crack tip. As suggested by Liechti and Chai [29], the measured fracture toughness G_c depends on contributions of intrinsic adhesive energy Γ_c, rate of plastic dissipation $\dot{W}_p$ near crack front, rate of bulk viscoelastic dissipation $\dot{W}_v$ and shielding/friction dissipation ΔG_c due to the interface roughness

$$G_c = \Gamma_c + \dot{W}_p + \dot{W}_v + \Delta G_c. \tag{5}$$

The values of $\dot{W}_p$, $\dot{W}_v$ and ΔG_c are maximized in pure shear and minimized in pure normal load cases. A numerical study of the dynamic delamination test by Tran *et al* [21] has indicated that the thin film delamination process is highly mixed-mode at the early stage of the failure process and gradually proceeds into a mode I dominant regime. The increase in the shear component at the early phase of the failure process, as a direct outcome of the increase in loading amplitude, not only enlarges the plastic zone [29] in the film (rate-dependent effect) but may also activate the interlocking of crack face asperities or toughening mechanism of the interface (mixed-mode effect) [30].

In a parametric study on the effect of the load pulse amplitude, Tran *et al* [21] have shown that an increasing portion of the imparted kinetic energy is transformed into bending strain energy in the film as the load level decreases. This observation suggests the need to exclude the strain energy from the total energy available for the failure process and the energy balance equation can be rewritten as

$$G_c = \frac{a_0 K_{1D} - U_f}{a_f - a_0}, \tag{6}$$

where U_f is the total strain energy per unit width stored in the film at the end of the failure process, i.e. at the time of crack arrest. The dependence of the total energy available for the failure process, $a_0 K_{1D} - U_f$, on the load level as pointed out in [21] also contributes to the apparent rate-dependent behaviour of the adhesion energy. This study has shown that for higher load amplitudes ($\simeq$1.5 GPa) more than 95% of total energy is channelled into the interfacial failure process. In contrast, only about 82% of the imparted energy is converted to the fracture energy at lower loading amplitudes ($\simeq$0.5 GPa). The influence of this energy transformation on the measured fracture toughness values (figure 10) is, however, less than other energy dissipated processes.

5. Conclusion

The interfacial fracture energy of an Al thin film on a Si substrate was extracted from a new laser-induced dynamic delamination protocol and compared with the value measured in a standard, quasi-static four-point bend test. In the dynamic experiment, an Al thin film was patterned on a Si Substrate with a weakly bonded region. This region essentially served as a pre-crack and effectively maximized the kinetic energy imparted to the film at the earlier stage of the fracture process, leading to successful interfacial crack extensions over several millimetres in length. Identical film strips were tested for increasing values of the stress pulse amplitude, which corresponded to an increase in peeling velocity and kinetic energy available for fracture. At low pulse amplitudes, the fracture energy was nearly constant and compared favourably with the value measured in the four-point bend test (2.5 J m^{-2}). As the pulse amplitude increased, an increase in fracture energy was observed, until reaching a plateau value of approximately 6 J m^{-2}. The dependence of fracture energy on pulse amplitude was attributed to rate and mixed-mode effects during the dynamic delamination process.

Acknowledgments

The authors gratefully acknowledge the support of the National Science Foundation (NSF) under Grant (CMMI 0726742), the Semiconductor Research Corporation Grant (SRC 2008 KJ1773), and a Vietnam Education Foundation (VEF) graduate fellowship. Experiments were carried out in part in the Frederick Seitz Materials Research Laboratory Central Facilities, University of Illinois, which are partially supported by the US Department of Energy under grants DE-FG02-07ER46453 and DE-FG02-07ER46471.

References

[1] Mittal K L 1987 Selected biliography on adhesion measurement of films and coatings *J. Adhes. Sci. Technol.* **1** 247–59
[2] Freund L B and Suresh S 2003 *Thin Film Materials: Stress, Defect Formation and Surface Evolution* (Cambridge: Cambridge University Press)
[3] Dauskardt R H, Lane H, Ma Q and Krishna N 1998 Adhesion and debonding of multi-layer thin film structures *Eng. Fract. Mech.* **61** 141–62
[4] Hartfield C D, Ogawa E T, Park Y J, Chiu T C and Guo H 2004 Interface reliability assessments for copper/low-k products *IEEE Trans. Device Mater. Reliab.* **4** 129–41
[5] Charalambides P G, Lund J and Evans A G 1989 A test specimen for determining the fracture resistance of bimaterial interfaces *J. Appl. Mech.* **56** 77–82
[6] Gupta V, Argon A S, Cornie J A and Parks D M 1990 Measurement of interface strength by laser pulse-induced spallation *Mater. Sci. Eng.* **126** 105–17
[7] Gupta V, Argon A S, Parks D M and Cornie J A 1992 Measurement of interface strength by a laser spallation technique *J. Mech. Phys. Solids* **40** 141–80
[8] Wang J 2002 Thin film adhesion measurement by laser induced stress waves *PhD Thesis* University of Illinois
[9] Wang J, Weaver R L and Sottos N R 2002 A parametric study of laser induced thin film spallation *Exp. Mech.* **42** 74–83
[10] Vossen J L 1978 Measurements of film–substrate bond strength by laser spallation ed K L Mittal Adhesion measurement of thin films, thick films and bulk coatings, ASTM STP 640 *Am. Soc. Test. Mater.* **640** 122–3
[11] Kandula S, Hartfield C D and Geubelle P H 2008 Adhesion strength measurement of polymer dielectric interfaces using laser spallation technique *Thin Solid Films* **516** 7627–35
[12] Kimberly J, Chasiotis I and Lambros J 2008 Failure of microelectromechanical systems subjected to impulse loads *Int. J. Solids Struct.* **45** 497–512
[13] Kitey R, Geubelle P and Sottos N 2009 Mixed-mode interfacial adhesive strength of a thin film on an anisotropic substrate *J. Mech. Phys. Solids* **57** 51–64
[14] Wang J, Weaver R L and Sottos N R 2004 Tensile and mixed-mode strength of a thin film–substrate interface under laser induced pulsed loading *J. Mech. Phys. Solids* **52** 999–1022
[15] Hu L and Wang J 2006 Pure-shear failure of thin films by laser-induced stress waves *Exp. Mech.* **46** 637–45
[16] Gupta V and Yuan J 1993 Measurement of interface strength by the modified laser-spallation technique: II. Applications to metal/ceramic interfaces *J. Appl. Phys.* **74** 2397–404
[17] Gupta V, Yuan J and Pronin A N 1994 Recent development in the laser spallation technique to measure the interface strength and its relationship to interface toughness with applications to metal/ceramic, ceramic/ceramic and ceramic/polymer interfaces *J. Adhes. Sci. Technol.* **8** 713–47
[18] Kandula S, Tran P, Geubelle P H and Sottos N R 2008 Dynamic delamination of patterned thin films *Appl. Phys. Lett.* **93** 261902
[19] Pronin A N and Gupta V 1998 Measurement of thin film interface toughness by using laser-generated stress pulses *J. Mech. Phys. Solids* **46** 389–410
[20] Tran P, Kandula S V, Geubelle P H and Sottos N R 2008 Hybrid spectral/finite element analysis of dynamic delamination of patterned thin films *Eng. Fract. Mech.* **75** 4217–33
[21] Tran P, Kandula S V, Geubelle P H and Sottos N R 2010 Dynamic delamination of patterned thin films: a numerical study *Int. J. Fract.* **162** 77–90
[22] Shaviv R, Roham S and Woytowitz P 2005 Optimizing the precision of the four-point bend test for the measurement of thin film adhesion *Microelectron. Eng.* **82** 99–112
[23] Lane H 2003 Interface fracture *Ann. Rev. Mater. Res.* **33** 29–54
[24] Hutchinson J W and Suo Z 1992 Mixed-mode cracking in layered material *Adv. Appl. Mech.* **29** 62–191
[25] Chaudhury M K 1999 Rate-dependent fracture at adhesive interface *J. Phys. Chem.* B **103** 6562–6
[26] Muralidhar S and Sunil S 2007 Scaling of fracture energy in tensile debonding of viscoelastic films *J. Appl. Phys.* **101** 093504

[27] Nguyen T, Govindjee S, Klein P and Gao H 2004 A rate-dependent cohesive continuum model for the study of crack dynamics *Comput. Methods Appl. Mech. Eng.* **193** 3239–65

[28] Nguyen T and Govindjee S 2006 Numerical study of geometric constraint and cohesive parameters in steady-state viscoelastic crack growth *Int. J. Fract.* **141** 255–68

[29] Liechti K M and Chai Y-S 1992 Asymmetric shielding in interfacial fracture under in-plane shear *J. Appl. Mech.* **59** 295–309

[30] Evans A G and Hutchinson J W 1989 Effects of non-planarity on the mixed-mode fracture resistance of bimaterial interfaces *Acta Mater.* **37** 909–16

[31] Thouless M D 1994 Fracture mechanics for thin film adhesion *IBM J. Res. Dev.* **38** 367–77